

Diagnostics for plasmon satellites and Hubbard bands in transition metal oxides

Steffen Backes^{1,2,3,*}, Hong Jiang⁴, and Silke Biermann^{3,5,6,7}

¹Research Center for Advanced Science and Technology,
University of Tokyo, Komaba, Tokyo 153-8904, Japan

²Center for Emergent Matter Science, RIKEN, Wako, Saitama 351-0198, Japan

³CPHT, CNRS, École polytechnique, Institut Polytechnique de Paris, 91120 Palaiseau, France

⁴College of Chemistry and Molecular Engineering, Peking University, China

⁵Collège de France, 11 place Marcelin Berthelot, 75005 Paris, France

⁶European Theoretical Spectroscopy Facility, 91128 Palaiseau, France, Europe and

⁷Department of Physics, Division of Mathematical Physics,
Lund University, Professorsgatan 1, 22363 Lund, Sweden

(Dated: January 13, 2023)

Coulomb correlations between the electrons imprint characteristic signatures to the spectral properties of materials. Among others, they are at the origin of a rich phenomenology of satellite features, either stemming from atomic-like multiplets or from interactions with particle-hole excitations or plasmons. While in many cases the latter lie at considerably higher energies than the former, suggesting clear distinction criteria, this picture has recently become blurred by indications that satellites of different types can coexist in the same energy range. It is now generally accepted that the identification of the nature of spectral features is a highly non-trivial task. In this article we propose a general procedure for tracing the origin of satellites of different types within modern *ab initio* calculations. As an illustration, we analyze the ternary transition metal oxides SrVO₃ and SrMoO₃, which are drosophila compounds for the coexistence of Hubbard and plasmonic satellites, reconciling previous seemingly contradictory findings in an unexpected manner.

INTRODUCTION

Impressive progress in direct – and to a much lesser extent inverse – photoemission spectroscopy over the last decades has resulted in a situation where the spectral properties of electronic systems have become some of the most commonly probed experimental properties of materials [1–3]. The main quantity is the spectral function $A(k, \omega)$, which encodes information about the possible electron removal and addition processes, as probed in direct and inverse photoemission. The knowledge of $A(k, \omega)$ in turn is typically synonymous with a good first understanding of the behaviour of the material under a variety of probes, even those not directly encoded in A .

In normal metals, the low-energy behaviour is governed by renormalized quasi-particle bands following the Landau Fermi liquid paradigm, while in insulators the spectrum is gapped around the Fermi level. Beyond these elementary considerations, spectral functions can however display a whole zoology of different features at intermediate or high energies (in typical transition metal oxides, in energy ranges spanning a few tenths to a few tens of eV).

Among the most prominent features in electronic systems with sizable Coulomb correlations are Hubbard satellites, remnants of the atomic physics in the material, corresponding to the atomic multiplets of an isolated atom placed in the crystal field environment of its surroundings but potentially acquiring some dispersion due

to the periodicity of the crystal. The energy scales of these multiplet structures are given by the effective local Coulomb interaction, often parametrized theoretically in the form of a local Hubbard U (or more precisely a Hubbard U matrix including Hund’s exchange and orbital structures) [4]. Such features have been studied in some detail in the past with elaborate theoretical approaches, starting from exact diagonalization[5, 6] and more recently within Dynamical Mean-Field Theory (DMFT)[7–9]. and are well-documented experimentally [6, 10].

Another type of satellites appearing in the spectral function of electronic materials are due to electrons coupling to plasmons [11–18]. Plasmons have been experimentally observed and theoretically investigated in materials ranging from elementary metals [19–21], bronzes[22, 23], oxides[18, 24–30], in particular ruthenates[31] and cuprates[32–34] as well as in graphene[16, 35, 36]. Plasmonic excitations are relevant and actively utilized in the design of functional materials[37–39], such as in plasmon-mediated photocatalysis[40, 41] and sensors[42]. Plasmons are collective electronic excitations, which are in general highly non-local in nature. They are encoded in the dielectric function describing the dynamic response of the electronic system as a whole to a perturbation. This response can be mediated by particle-hole excitations as well as by collective (plasmonic) excitations, which both can give rise to shake-up satellites in the spectral function. For simplicity, below, we will refer to any features beyond a local atomic-like picture, i.e. originating

from non-local collective excitations as plasmonic satellites, and our aim will be to distinguish those from the Hubbard-type satellites described above. This differentiation becomes non-trivial when the energy scale of plasmonic excitations is similar to that of the local Coulomb interactions, which can lead to both Hubbard and plasmon satellites to appear at similar energies. Recently, evidence has accumulated that this is the case in a large number of transition metal oxides [43–51].

In this letter we present a protocol for a quantitative *ab initio* identification of Hubbard and plasmonic contributions in low-energy satellites in real materials. Using this protocol, we reinvestigate two prototypical 3d and 4d perovskite transition metal oxides, SrVO₃ and SrMoO₃, and determine the Hubbard and plasmonic contributions in the observed low-energy satellites. Contrary to previous interpretations [48–51], we find both Hubbard and plasmon satellites to be present, albeit with different magnitude. On the other hand, our findings reconcile seemingly contradictory calculations within many-body perturbation theory (within the GW approximation) and combined GW+Dynamical Mean Field Theory (GW+DMFT) in a surprising manner.

SrVO₃ is a 3d¹ compound with metallic V *t*_{2g} states crossing the Fermi level, forming a typical 3-peak structure in the spectral function, both confirmed from experiment [52–57] and theoretical calculations [53, 54, 57–60]. The proposed origin of the satellites though has significantly evolved over the years. Early combined density functional theory and dynamical mean-field theory (DFT+DMFT) calculations suggested that the satellites arise from strong local V-*t*_{2g} Coulomb interactions in the form of Hubbard bands [53, 54, 58, 59, 61–63]. The advent of combined many-body perturbation theory and dynamical mean field theory (“GW+DMFT”) [64], however, made it possible to include both, Hubbard bands and plasmonic features, in the theoretical description, and it was realized that in the low energy (< 5 eV) range features of both types can coexist [60, 65]. Moreover, it was pointed out that the empty V-*e*_g states that are split off from the partially filled V-*t*_{2g} states by the octahedral crystal field lie in the same energy range as the upper Hubbard band from the early DFT+DMFT calculations. Interestingly, many-body perturbation theory alone could also reproduce the observed satellite features (albeit at slightly shifted energetic positions) [47], a finding which seemed to be in contradiction with the interpretation as Hubbard bands. Along this line, several works [47–51] gave a purely plasmonic interpretation to the lowest energy features both in the occupied and the unoccupied part of the spectrum. A new twist appeared when it was realized that oxygen vacancies contribute spectral weight at the same energy as the satellite in the occupied spectrum [57]. While the importance of oxygen vacancies responsible for part of the spectral weight in the energy range in question is now widely recognized,

no consensus has been reached so far concerning the origin of the remaining intrinsic part of the satellite.

We now turn to a brief discussion of the theoretical description of the creation of plasmonic features in the spectral function, within DMFT-derived schemes. As is well-known [13, 15, 48, 60, 64, 66–68] electronic screening is a dynamical process, since the response of the electronic density in a solid to a perturbation depends on the energy scale of the perturbation. For a given set of orbitals of interest, the charge redistribution and thus the screening is energy dependent, and directly translates into the notion of a frequency-dependent effective screened Coulomb interaction $U(\omega)$ when higher energy degrees of freedom are integrated out [66]. An approximate form of the effective $U(\omega)$ can be obtained for example within the constrained Random-Phase-Approximation (cRPA) [13, 66], that considers only screening processes outside of a target low-energy subspace. From $U(\omega)$ two important pieces of physical information can be deduced: First, the value of the static screened interaction $U(\omega = 0)$, determining in an atomic picture the energetic positions of the atomic multiplets, which in a periodic crystal typically result in non- or weakly dispersive broad satellites, the *Hubbard bands*. Second, the crossover from the screened to the bare Coulomb interaction at the plasma frequency ω_0 creates satellites from collective electron excitations at multiples of ω_0 [15].

In oxides with different manifolds of bands (e.g. corresponding to the *d*- or *p*- states), additional “subplasmons” corresponding to collective excitations within specific subspaces of the full Hilbert space can occur. For SrVO₃, for example, besides the main plasmon (located at $\omega_0 \approx 14.5$ eV) multiple excitations are found in the dielectric function, namely around 2.5 eV and 5 eV, the former originating from charge-oscillations in the V *t*_{2g} manifold [47, 60, 65]. This is precisely the energy scale where Hubbard satellites have been reported in SrVO₃ [53, 54, 58, 59], indicating that both plasmonic and Hubbard satellite features may exist in this system, and at comparable energies.

Different state-of-the-art methods usually obtain only a partial picture of the satellites, as shown in Fig. 1. Compared to a Density-Functional-Theory (DFT) calculation, which neither can describe Hubbard or plasmonic satellites, the consideration of dynamical screening processes within the *GW* approximation introduces plasmonic satellites in the occupied and unoccupied part of the spectrum. Including the effects of correlations originating from the low-energy part $U(\omega = 0)$ of the Coulomb interaction but without dynamical screening within DFT+DMFT, one also observes satellites at very similar energies but now of Hubbard-type origin. This hints at a possible coexistence of both features in the final spectrum, but necessitates the use of a method that treats both Hubbard and plasmon contributions on equal footing, like the combination of *GW* and DMFT

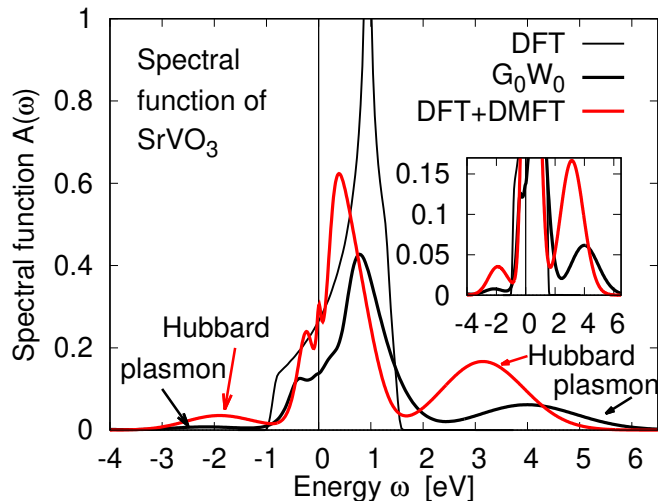


FIG. 1: The spectral function of SrVO₃, calculated within Density Functional Theory (DFT), the G_0W_0 approximation and a low-energy model solved in DFT+Dynamical Mean-Field Theory (DFT+DMFT). The G_0W_0 approximation introduces corrections due to dynamical screening effects and plasmon satellites, while DFT+DMFT describes low-energy correlations and the emergence of Hubbard bands. The inset shows the same data on a smaller scale.

($GW+EDMFT$)[48, 49, 60, 64, 65]. In this method non-local correlation and screening processes are accounted for by the GW approximation, while the local part is obtained from the DMFT solution of a local impurity problem subject to the partially screened interaction $U(\omega)$, which encodes all screening processes beyond the low-energy subspace in its frequency dependence. Since Hubbard satellites originate from the low-energy part $U(\omega = 0)$, and plasmons from dynamical screening, i.e. they emerge in the local model via the frequency dependence of $U(\omega)$, we can use this to disentangle their contributions. Using $GW+EDMFT$ in its causal implementation[69], we propose the following protocol to identify and separate out only the plasmonic contributions in the spectral function: The effective Coulomb interaction $U(\omega)$ can be artificially reduced by a constant shift such that the static effective Coulomb interaction $U(\omega = 0)$ vanishes, but the full frequency dependence is retained. This removes contributions from low-energy correlations, *i.e.* the Hubbard satellites, but fully retains the plasmonic contribution. (See appendix for a one-orbital proof-of-principle example.)

The resulting spectral function for SrVO₃ within this scheme is shown in Fig. 2. Without any artificial reduction of the interaction the result is very similar to previous $GW+EDMFT$ calculations[48, 49, 60], with a renormalized quasi-particle peak and a main satellite in the occupied and unoccupied part. Different from DMFT but similar as in GW [47, 70] one observes an additional plasmon satellite around -5 eV, originating from tran-

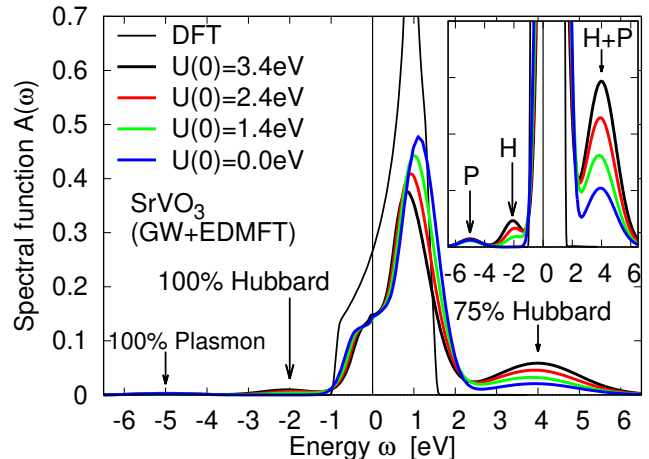


FIG. 2: The spectral function of SrVO₃ for different values of the screened static interaction $U(0)$ as obtained from $GW+DMFT$, including both Hubbard- and plasmonic physics. The low-energy satellite in the occupied part of the spectrum vanishes for $U(0) = 0$ eV, indicating it is purely composed of a Hubbard satellite. On the other hand, the upper satellite is composed of $\sim 25/75\%$ plasmonic/Hubbard weight.

sitions outside the t_{2g} space[47]. Reducing the static interaction from the *ab initio* value $U(0) = 3.4$ eV to zero, we observe, besides an expected increase in bandwidth, a strong reduction of the two satellites closest to the Fermi level, where the lower satellite completely vanishes for $U(0) = 0$ eV. A small upper satellite remains with about 25% of the original weight. The satellite at -5 eV is not affected. This indicates that the satellite around -2 eV in SrVO₃ is indeed purely a lower Hubbard band, albeit with an intensity lower than reported in DFT+DMFT. This in fact agrees with the experimental observation that the lower intrinsic satellite is rather small and in general contains significant contributions from oxygen vacancies[57]. On the other hand, the remaining satellites around ± 5 eV correspond to the plasmon satellites in SrVO₃ originating from the 5 eV transition reported in the energy loss function of SrVO₃[47, 60, 65]. The upper satellite is thus composed of Hubbard ($\sim 75\%$) and plasmonic ($\sim 25\%$) contributions at similar energies, with the plasmon satellite effectively 'buried' beneath the dominant Hubbard satellite.

Eventually the $GW+EDMFT$ spectral function and its satellites are very similar to the G_0W_0 result, except for a slight increase in renormalization (see appendix for a direct comparison), in contrast to previous results[48, 49], which found a reduction in correlation. This difference stems from causality violations in the previous computational scheme, as discussed in Ref[69], whereas our current scheme does not suffer from this issue. This agreement between G_0W_0 and $GW+EDMFT$ not only indicates that the current level of self-consistency is suffi-

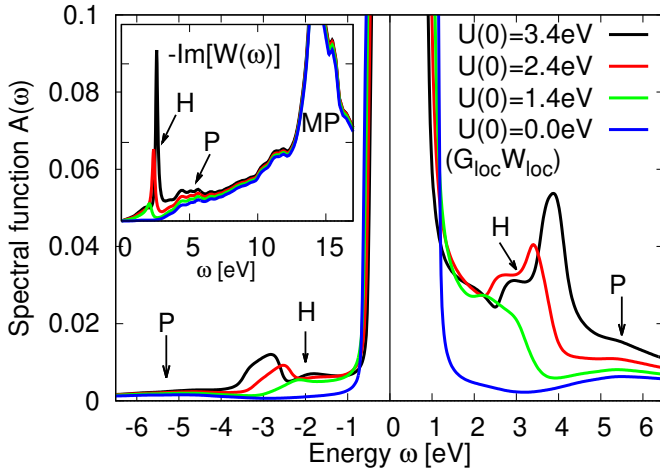


FIG. 3: The t_{2g} spectral function of SrVO₃ obtained from a local G_0W_0 approximation for different values of the screened interaction $U(0)$ but retaining the full frequency dependence. The inset shows the negative imaginary part of the resulting fully screened interaction $W(\omega)$. The lower and upper Hubbard (H)-like peaks originate from a local charge oscillation in the t_{2g} orbitals, corresponding to the peak around 2.5 eV in $W(\omega)$. As in Fig.2 these satellites vanish when the screened static interaction $U(0)$ becomes zero, and only the plasmon contribution (P) remains. (MP) indicates the main plasmon excitation.

cient, but also that SrVO₃ is only moderately correlated such that G_0W_0 is able to capture most of the relevant physics. Therefore, the interpretation of the low-energy satellites as Hubbard satellites in SrVO₃ raises the question about the true nature of the G_0W_0 low-energy satellites. As they originate from charge excitations in the vanadium t_{2g} manifold[47, 60], we apply a similar local G_0W_0 scheme to disentangle possible collective non-local charge excitations (plasmons) from local Hubbard-like physics. In Fig. 3 we show the resulting spectral function $A(\omega)$ and screened interaction $W(\omega)$ for SrVO₃ within a local low-energy G_0W_0 scheme. In this scheme the local 'bare' $V t_{2g}$ interaction $U(\omega)$ is screened by only considering local transitions in the t_{2g} space, and the resulting $W(\omega)$ is convoluted with the local non-interacting t_{2g} Green's function to obtain the effective self-energy (i.e., the impurity model is solved within the G_0W_0 approximation). The resulting $W(\omega)$ and spectral function almost perfectly reproduces the full G_0W_0 calculation, besides an overestimation of the energetic position of the t_{2g} derived peak in $W(\omega)$ around 3 eV, which leads to an overestimation of the satellite position. As the calculation has been performed on the real frequency axis, more pronounced structures are visible and not smeared out by the analytic continuation procedure. This result indicates that the low-energy peaks in G_0W_0 can be explained by only considering local charge excitations and a local Coulomb interaction. Similarly as for

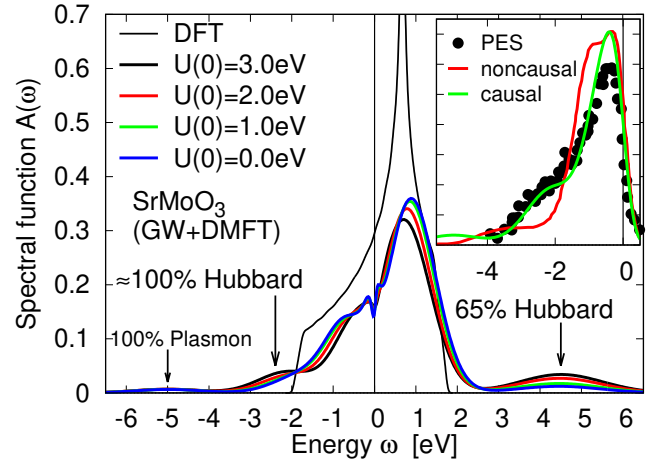


FIG. 4: The spectral function of SrMoO₃ for different values of the screened static interaction $U(0)$ as obtained from $GW+EDMFT$. The low-energy satellite around -2.5 eV is mostly composed of a Hubbard satellite, while the unoccupied satellite is about 35% plasmonic and 65% Hubbard type origin. The inset shows the same spectral function at $U = 3$ eV, compared to a noncausal implementation (taken from [49]) and photoemission data (taken from [71]).

the $GW+EDMFT$ result, the peaks vanish as the static screened interaction is reduced, confirming their local 'Hubbard'-like nature. Even though G_0W_0 as a perturbative approach cannot access strong electronic correlations, the corresponding atomic multiplet excitations are effectively encoded in $W(\omega)$ via the RPA approximation and give rise to satellites representing the Hubbard satellites obtained in non-perturbative methods. Thus, this result confirms that the low-energy satellites in SrVO₃ do not originate from non-local collective excitations but arise purely from local Hubbard-like charge excitations given by the static local interaction $U(\omega = 0)$. Plasmon satellites are only found at energies (and beyond) ± 5 eV.

We apply the same method to the closely related $4d^2$ material SrMoO₃, which is isostructural to SrVO₃. Due to the more extended nature of the $4d$ orbitals, low-energy electronic correlations are weaker and the experimentally observed satellites have been proposed to be of purely plasmonic origin[49, 71–73]. The resulting spectral function for different values of the static interaction is shown in Fig. 4. As in previous reports we obtain a much broader quasiparticle peak than in SrVO₃, with a lower shoulder-like feature around 2.5 eV and an upper satellite. Upon reducing the static interaction, we see a similar trend as in SrVO₃, but less pronounced. For $U(0) = 0$ the occupied shoulder seems to completely merge with the quasiparticle peak, corresponding to a Hubbard satellite, but we found the analytic continuation procedure to be less reliable in that area. The existence of a small lower Hubbard satellite does not contradict with a previous DFT+DMFT study[72], which

found no pronounced Hubbard satellite but still a significant amount of spectral weight shifted to lower energies around -2.5 eV, very similar to our results. The unoccupied satellite is significantly reduced, retaining about 35% of its weight as a plasmon satellite. Similar as in SrVO₃, we find that SrMoO₃ shows pronounced plasmon satellites around ± 5 eV. Most noteworthy, the causal implementation of $GW+EDMFT$ used in this manuscript is able to accurately reproduce the observed experimental spectral function from photoemission experiments[71], demonstrating that this approach is capable of capturing the relevant physics in this material and thus strengthening our interpretation of the spectral features as Hubbard satellites. The noncausal formulation[49] shows a significantly lower intensity for the Hubbard-like satellite and increased bandwidth of the V t_{2g} quasi-particle dispersive states, indicating that the noncausal variant underestimates the electronic correlation strength also in SrMoO₃, in line with previous observations[69, 74].

In summary, we have revisited the decade-old problem of the nature of spectral satellites in ternary transition metal oxides, and proposed a theoretical *ab initio* method to distinguish plasmonic satellites, which emerge from collective electronic excitations, from Hubbard-type satellites, resulting from a strong local Coulomb interaction. For the prototypical transition metal oxide SrVO₃ we show that the occupied low-energy satellite is purely composed of Hubbard-type incoherent weight, while in the unoccupied satellite both Hubbard and plasmonic contributions coexist at similar energies. In the weaker correlated $4d^2$ SrMoO₃ we observe a similar but less pronounced picture of a Hubbard satellite in the occupied part, and both plasmon and Hubbard satellites at similar energies in the unoccupied part. These observations call for a reinvestigation of similar and other correlated materials and their satellite features, both theoretically and experimentally, as they are in particular relevant for plasmon-mediated applications in functional materials, where precise knowledge of the intensity and energy of plasmonic excitations is needed. The scheme that we have developed can be applied to a large class of materials, and can aid the development of such applications by theoretically quantifying the plasmonic and Hubbard-type contributions in the spectral satellites.

While this work was being prepared for publication, a new joint experimental-theoretical work appeared on SrVO₃[75]. In that work, a purely plasmonic origin of the satellites is advocated. However, we believe this apparent contradiction also to be resolved by our work, since we show that the corresponding features stem indeed from the dielectric function, but are nevertheless of multiplet-like origin rather than long-range collective excitations, see discussion above.

The authors gratefully acknowledge fruitful discussions with F. Aryasetiawan, M. Gatti, A. Lichtenstein, L. Reininger and G. Sawatzky. This work was supported by a

Consolidator Grant of the European Research Council (Project CorrelMat-617196) and GENCI/IDRIS Orsay under project A0130901393.

* steffen-backes@g.ecc.u-tokyo.ac.jp

- [1] A. Damascelli, Physica Scripta Volume T **109**, 10.1238/Physica.Topical.109a00061 (2004).
- [2] J. A. Sobota, Y. He, and Z.-X. Shen, Rev. Mod. Phys. **93**, 025006 (2021).
- [3] H. Zhang, T. Pincelli, C. Jozwiak, T. Kondo, R. Ernstorfer, T. Sato, and S. Zhou, Nature Reviews Methods Primers **2**, 10.1038/s43586-022-00133-7 (2022).
- [4] J. Hubbard, Proceedings of the Royal Society of London A: Mathematical, Physical and Engineering Sciences **276**, 238 (1963), <http://rspa.royalsocietypublishing.org/content/276/1365/238.full.pdf>
- [5] D. van der Marel and G. A. Sawatzky, Phys. Rev. B **37**, 10674 (1988).
- [6] J. Zaanen and G. A. Sawatzky, Progress of Theoretical Physics Supplement **101**, 231 (1990), <https://academic.oup.com/ptps/article-pdf/doi/10.1143/PTP.101.231/5450560/101-231.pdf>
- [7] V. I. Anisimov, A. I. Poteryaev, M. A. Korotin, A. O. Anokhin, and G. Kotliar, Journal of Physics: Condensed Matter **9**, 7359 (1997).
- [8] A. I. Lichtenstein and M. I. Katsnelson, Phys. Rev. B **57**, 6884 (1998).
- [9] G. Kotliar, S. Y. Savrasov, K. Haule, V. S. Oudovenko, O. Parcollet, and C. A. Marianetti, Rev. Mod. Phys. **78**, 865 (2006).
- [10] B. T. Thole, G. van der Laan, J. C. Fuggle, G. A. Sawatzky, R. C. Karnatak, and J.-M. Esteve, Phys. Rev. B **32**, 5107 (1985).
- [11] J.-J. Chang and D. C. Langreth, Phys. Rev. B **5**, 3512 (1972).
- [12] J.-J. Chang and D. C. Langreth, Phys. Rev. B **8**, 4638 (1973).
- [13] F. Aryasetiawan, M. Imada, A. Georges, G. Kotliar, S. Biermann, and A. I. Lichtenstein, Phys. Rev. B **70**, 195104 (2004).
- [14] M. Guzzo, G. Lani, F. Sottile, P. Romaniello, M. Gatti, J. J. Kas, J. J. Rehr, M. G. Silly, F. Sirotti, and L. Reininger, Phys. Rev. Lett. **107**, 166401 (2011).
- [15] M. Casula, P. Werner, L. Vaugier, F. Aryasetiawan, T. Miyake, A. J. Millis, and S. Biermann, Phys. Rev. Lett. **109**, 126408 (2012).
- [16] J. Lischner, D. Vigil-Fowler, and S. G. Louie, Phys. Rev. Lett. **110**, 146801 (2013).
- [17] C. Lemell, S. Neppel, G. Wachter, K. Tórkési, R. Ernstorfer, P. Feulner, R. Kienberger, and J. Burgdörfer, Phys. Rev. B **91**, 241101 (2015).
- [18] F. Borgatti, J. A. Berger, D. Céolin, J. S. Zhou, J. J. Kas, M. Guzzo, C. F. McConville, F. Offi, G. Panaccione, A. Regoutz, D. J. Payne, J.-P. Rueff, O. Bierwagen, M. E. White, J. S. Speck, M. Gatti, and R. G. Egdell, Phys. Rev. B **97**, 155102 (2018).
- [19] K. Karlsson and F. Aryasetiawan, Phys. Rev. B **52**, 4823 (1995).

- [20] F. Aryasetiawan, L. Hedin, and K. Karlsson, *Phys. Rev. Lett.* **77**, 2268 (1996).
- [21] P. Steiner, H. Höchst, and S. Hüfner, *Zeitschrift für Physik B Condensed Matter* **30**, 129 (1978).
- [22] M. Campagna, G. K. Wertheim, H. R. Shanks, F. Zumbach, and E. Banks, *Phys. Rev. Lett.* **34**, 738 (1975).
- [23] J. N. Chazalviel, M. Campagna, G. K. Wertheim, and H. R. Shanks, *Phys. Rev. B* **16**, 697 (1977).
- [24] N. Beatham, P. Cox, R. Egdell, and A. Orchard, *Chemical Physics Letters* **69**, 479 (1980).
- [25] F. Aryasetiawan and O. Gunnarsson, *Phys. Rev. Lett.* **74**, 3221 (1995).
- [26] R. G. Egdell, J. Rebane, T. J. Walker, and D. S. L. Law, *Phys. Rev. B* **59**, 1792 (1999).
- [27] V. Christou, M. Etchells, O. Renault, P. J. Dobson, O. V. Salata, G. Beamson, and R. G. Egdell, *Journal of Applied Physics* **88**, 5180 (2000), <https://doi.org/10.1063/1.1312847>.
- [28] S. Kohiki, M. Arai, H. Yoshikawa, S. Fukushima, M. Oku, and Y. Waseda, *Phys. Rev. B* **62**, 7964 (2000).
- [29] M. Gatti, F. Bruneval, V. Olevano, and L. Reining, *Phys. Rev. Lett.* **99**, 266402 (2007).
- [30] J. J. Mudd, T.-L. Lee, V. Muñoz Sanjosé, J. Zúñiga Pérez, D. Hesp, J. M. Kahk, D. J. Payne, R. G. Egdell, and C. F. McConville, *Phys. Rev. B* **89**, 035203 (2014).
- [31] P. Cox, J. Goodenough, P. Tavener, D. Telles, and R. Egdell, *Journal of Solid State Chemistry* **62**, 360 (1986).
- [32] I. Bozovic, *Phys. Rev. B* **42**, 1969 (1990).
- [33] D. van der Marel, *Journal of Superconductivity* **17**, 559 (2004).
- [34] P. Werner, R. Sakuma, F. Nilsson, and F. Aryasetiawan, *Phys. Rev. B* **91**, 125142 (2015).
- [35] X. Luo, T. Qiu, W. Lu, and Z. Ni, *Materials Science and Engineering: R: Reports* **74**, 351 (2013).
- [36] M. Guzzo, J. J. Kas, L. Sponza, C. Giorgetti, F. Sottile, D. Pierucci, M. G. Silly, F. Sirotti, J. J. Rehr, and L. Reining, *Phys. Rev. B* **89**, 085425 (2014).
- [37] B. Raveau, *Journal of the European Ceramic Society* **25**, 1965 (2005), *electroceramics IX*.
- [38] F. Cheng, J. Liang, Z. Tao, and J. Chen, *Advanced Materials* **23**, 1695 (2011), <https://onlinelibrary.wiley.com/doi/pdf/10.1002/adma.201003587>.
- [39] N. Nuraje, R. Asmatulu, and S. Kudaibergenov, *Current Inorganic Chemistry* **2**, 124 (2012).
- [40] W. Hou and S. B. Cronin, *Advanced Functional Materials* **23**, 1612 (2013), <https://onlinelibrary.wiley.com/doi/pdf/10.1002/adfm.201202148>.
- [41] X. Meng, L. Liu, S. Ouyang, H. Xu, D. Wang, N. Zhao, and J. Ye, *Advanced Materials* **28**, 6781 (2016), <https://onlinelibrary.wiley.com/doi/pdf/10.1002/adma.201603505>.
- [42] S. Szunerits and R. Boukherroub, *Chem. Commun.* **48**, 8999 (2012).
- [43] Y. Y. Wang, F. C. Zhang, V. P. Dravid, K. K. Ng, M. V. Klein, S. E. Schnatterly, and L. L. Miller, *Phys. Rev. Lett.* **77**, 1809 (1996).
- [44] H. Makino, I. H. Inoue, M. J. Rozenberg, I. Hase, Y. Aiura, and S. Onari, *Phys. Rev. B* **58**, 4384 (1998).
- [45] A. P. Grosvenor, M. C. Biesinger, R. S. Smart, and N. S. McIntyre, *Surface Science* **600**, 1771 (2006).
- [46] R. S. Markiewicz and A. Bansil, *Phys. Rev. B* **75**, 020508 (2007).
- [47] M. Gatti and M. Guzzo, *Phys. Rev. B* **87**, 155147 (2013).
- [48] L. Boehnke, F. Nilsson, F. Aryasetiawan, and P. Werner, *Phys. Rev. B* **94**, 201106(R) (2016).
- [49] F. Nilsson, L. Boehnke, P. Werner, and F. Aryasetiawan, *Phys. Rev. Materials* **1**, 043803 (2017).
- [50] F. Petocchi, F. Nilsson, F. Aryasetiawan, and P. Werner, *Phys. Rev. Research* **2**, 013191 (2020).
- [51] C.-N. Yeh, S. Isakov, D. Zgid, and E. Gull, *Phys. Rev. B* **103**, 195149 (2021).
- [52] I. H. Inoue, I. Hase, Y. Aiura, A. Fujimori, Y. Haruyama, T. Maruyama, and Y. Nishihara, *Phys. Rev. Lett.* **74**, 2539 (1995).
- [53] M. J. Rozenberg, I. H. Inoue, H. Makino, F. Iga, and Y. Nishihara, *Phys. Rev. Lett.* **76**, 4781 (1996).
- [54] A. Sekiyama, H. Fujiwara, S. Imada, S. Suga, H. Eisaki, S. I. Uchida, K. Takegahara, H. Harima, Y. Saitoh, I. A. Nekrasov, G. Keller, D. E. Kondakov, A. V. Kozhevnikov, T. Pruschke, K. Held, D. Vollhardt, and V. I. Anisimov, *Phys. Rev. Lett.* **93**, 156402 (2004).
- [55] M. Takizawa, M. Minohara, H. Kumigashira, D. Toyota, M. Oshima, H. Wadati, T. Yoshida, A. Fujimori, M. Lippmaa, M. Kawasaki, H. Koinuma, G. Sordi, and M. Rozenberg, *Phys. Rev. B* **80**, 235104 (2009).
- [56] S. Aizaki, T. Yoshida, K. Yoshimatsu, M. Takizawa, M. Minohara, S. Ideta, A. Fujimori, K. Gupta, P. Mahadevan, K. Horiba, H. Kumigashira, and M. Oshima, *Phys. Rev. Lett.* **109**, 056401 (2012).
- [57] S. Backes, T. C. Rödel, F. Fortuna, E. Frantzeskakis, P. Le Fèvre, F. Bertran, M. Kobayashi, R. Yukawa, T. Mitsubashi, M. Kitamura, K. Horiba, H. Kumigashira, R. Saint-Martin, A. Fouchet, B. Berini, Y. Dumont, A. J. Kim, F. Lechermann, H. O. Jeschke, M. J. Rozenberg, R. Valentí, and A. F. Santander-Syro, *Phys. Rev. B* **94**, 241110 (2016).
- [58] E. Pavarini, S. Biermann, A. Poteryaev, A. I. Lichtenstein, A. Georges, and O. K. Andersen, *Phys. Rev. Lett.* **92**, 176403 (2004).
- [59] B. Amadon, F. Lechermann, A. Georges, F. Jollet, T. O. Wehling, and A. I. Lichtenstein, *Phys. Rev. B* **77**, 205112 (2008).
- [60] J. M. Tomczak, M. Casula, T. Miyake, and S. Biermann, *Phys. Rev. B* **90**, 165138 (2014).
- [61] A. Liebsch, *Phys. Rev. Lett.* **90**, 096401 (2003).
- [62] I. A. Nekrasov, G. Keller, D. E. Kondakov, A. V. Kozhevnikov, T. Pruschke, K. Held, D. Vollhardt, and V. I. Anisimov, *Phys. Rev. B* **72**, 155106 (2005).
- [63] I. A. Nekrasov, K. Held, G. Keller, D. E. Kondakov, T. Pruschke, M. Kollar, O. K. Andersen, V. I. Anisimov, and D. Vollhardt, *Phys. Rev. B* **73**, 155112 (2006).
- [64] S. Biermann, F. Aryasetiawan, and A. Georges, *Phys. Rev. Lett.* **90**, 086402 (2003).
- [65] J. M. Tomczak, M. Casula, T. Miyake, F. Aryasetiawan, and S. Biermann, *EPL (Europhysics Letters)* **100**, 67001 (2012).
- [66] F. Aryasetiawan, K. Karlsson, O. Jepsen, and U. Schönberger, *Phys. Rev. B* **74**, 125106 (2006).
- [67] M. Casula, A. Rubtsov, and S. Biermann, *Phys. Rev. B* **85**, 035115 (2012).
- [68] L. Reining, *WIREs Computational Molecular Science* **8**, e1344 (2018), <https://wires.onlinelibrary.wiley.com/doi/pdf/10.1002/wcms.1344>.
- [69] S. Backes, J.-H. Sim, and S. Biermann, *Phys. Rev. B*

- 105**, 245115 (2022).
- [70] K. Nakamura, Y. Nohara, Y. Yosimoto, and Y. Nomura, *Phys. Rev. B* **93**, 085124 (2016).
- [71] A. Ali, B. H. Reddy, and R. S. Singh, *AIP Conference Proceedings* **2115**, 030389 (2019), <https://aip.scitation.org/doi/pdf/10.1063/1.5113228>.
- [72] H. Wadati, J. Mravlje, K. Yoshimatsu, H. Kumigashira, M. Oshima, T. Sugiyama, E. Ikenaga, A. Fujimori, A. Georges, A. Radetinac, K. S. Takahashi, M. Kawasaki, and Y. Tokura, *Phys. Rev. B* **90**, 205131 (2014).
- [73] A. Radetinac, J. Zimmermann, K. Hoyer, H. Zhang, P. Komissinskiy, and L. Alff, *Journal of Applied Physics* **119**, 055302 (2016), <https://doi.org/10.1063/1.4940969>.
- [74] J. Chen, F. Petocchi, and P. Werner, *Phys. Rev. B* **105**, 085102 (2022).
- [75] C.-P. Su, K. Ruotsalainen, A. Nicolaou, M. Gatti, and A. Gloter, *Advanced Optical Materials* **n/a**, 2202415 (2023), <https://onlinelibrary.wiley.com/doi/pdf/10.1002/adom.202202415>.

Diagnosics for plasmon satellites and Hubbard bands in transition metal oxides - Supplementary Material

Steffen Backes^{1,2,3,*}, Hong Jiang⁴, and Silke Biermann^{3,5,6,7}

¹Research Center for Advanced Science and Technology,
University of Tokyo, Komaba, Tokyo 153-8904, Japan

²Center for Emergent Matter Science, RIKEN, Wako, Saitama 351-0198, Japan

³CPHT, CNRS, École polytechnique, Institut Polytechnique de Paris, 91120 Palaiseau, France

⁴College of Chemistry and Molecular Engineering, Peking University, China

⁵Collège de France, 11 place Marcelin Berthelot, 75005 Paris, France

⁶European Theoretical Spectroscopy Facility, 91128 Palaiseau, France, Europe and

⁷Department of Physics, Division of Mathematical Physics,
Lund University, Professorsgatan 1, 22363 Lund, Sweden

(Dated: January 13, 2023)

COMPUTATIONAL DETAILS

For the GW+EDMFT cycle we start with a well converged DFT calculation from Wien2K [1], and perform a constrained Random-Phase-Approximation and a G_0W_0 calculation, as implemented in the FHI-gap Code[2], to obtain the effective impurity interaction $U(\omega)$ and the Selfenergy $\Sigma_{GW}(k, i\omega_n)$, projected onto the t_{2g} orbitals of either SrVO₃ or SrMoO₃, using a maximally localized Wannier basis. The cRPA and GW calculation were performed on a $8 \times 8 \times 8$ k-mesh, and the resulting $U(\omega)$ and $\Sigma_{GW}(k, i\omega_n)$ are then interpolated by cubic interpolation onto a dense $30 \times 30 \times 30$ k-mesh, which serves as the input for the selfconsistent EDMFT calculation. The impurity model is solved within the continuous-time Quantum Monte-Carlo method in the hybridization expansion, as implemented in the ALPS package[3] at inverse temperature $\beta = 40$ 1/eV, including the frequency dependence of the monopole term $F_0(\omega)$ of the effective interaction. The analytical continuation from the imaginary to the real frequency axis is done using a combination of Padé approximants and the Maximum Entropy code from Ref. [4], where we added plasmonic peaks in the default model of exponentially decaying weight at multiples of the plasma frequency to facilitate proper continuation.

The GW+EDMFT calculation was not done fully self-consistently, i.e. the nonlocal GW self-energy remained at the G_0W_0 level, and the effective interaction $U(i\omega)$ was not updated. As discussed in the main text the resulting spectral function from this GW+EDMFT is very close to the G_0W_0 result, as shown in Fig.1. This indicates that further self-consistency will have only minor effects and not qualitatively change the one-shot result. Therefore, we only considered the 'one-shot' GW+EDMFT results, which are computationally less demanding.

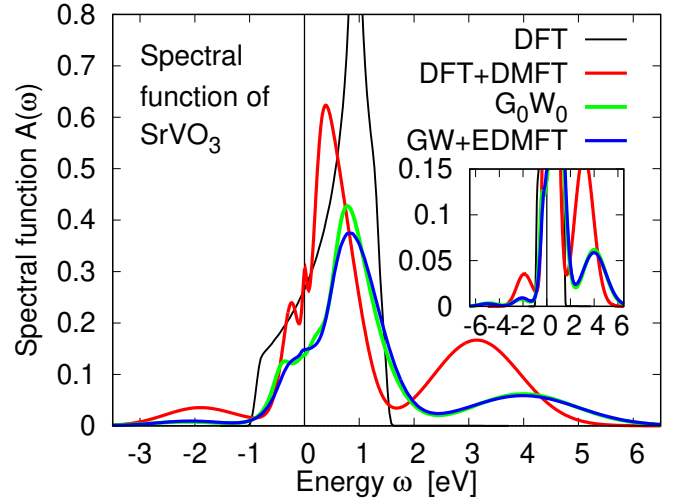


FIG. 1: The spectral function of SrVO₃, comparing the Density Functional Theory (DFT), the DFT+DMFT, the G_0W_0 approximation and the GW+EDMFT result shown in the main text. The G_0W_0 and the GW+EDMFT spectral functions are almost identical, indicating that a fully selfconsistent GW+EDMFT calculation will not significantly change the result.

LOCAL G_0W_0 AND SATELLITES

The results shown in Fig. 3 in the main text were obtained by employing a local G_0W_0 approximation: First, the polarization was calculated from the projected local DFT Green's function for the t_{2g} orbitals as $P_{loc} = G_{loc}G_{loc}$. For the effective "bare" interaction the cRPA derived impurity interaction $U(\omega)$ was used, which was screened by the local polarization to obtain the screened local interaction $W_{loc} = U[1 - P_{loc}U]^{-1}$ (shown in the inset of Fig. 3 in the main text). Then the self-energy was obtained by the convolution of the local Green's function and screened interaction as $\Sigma = G_{loc}W_{loc}$.

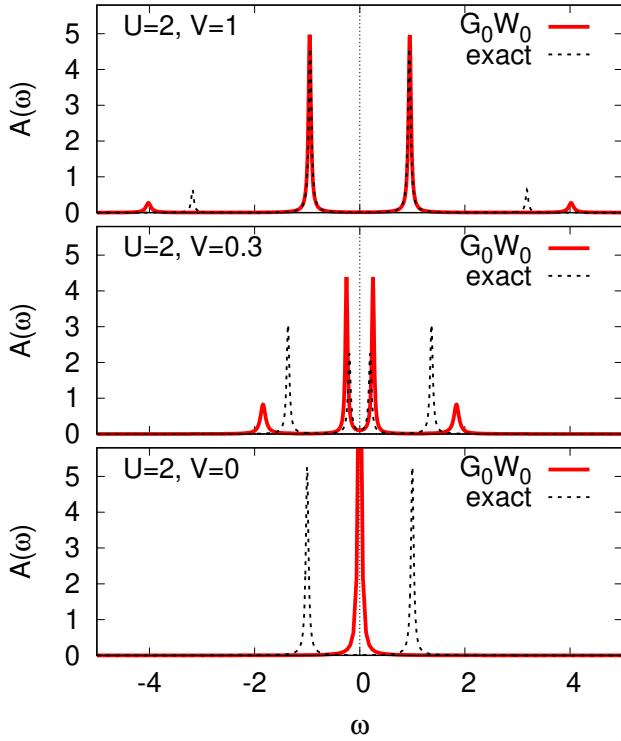


FIG. 2: The ground state spectral function for a DMFT impurity model with one bath site solved within the G_0W_0 approximation for different values of the hybridization strength V at fixed interaction $U = 2$. Except in the strong interaction limit $V \rightarrow 0$ G_0W_0 captures all qualitative features and correlation satellites, albeit overestimating their energetic position.

To elucidate the appearance of the Hubbard correlation satellites within G_0W_0 one can consider a simplified ‘linearized’ DMFT impurity problem [5–7] with only one bath site, which can be solved analytically

$$H = U n_{\uparrow} n_{\downarrow} + V \sum_{\sigma} (c_{\sigma}^{\dagger} f_{\sigma} + f_{\sigma}^{\dagger} c_{\sigma}) - \mu \sum_{\sigma} n_{\sigma}, \quad (1)$$

with $c, c^{\dagger}/f, f^{\dagger}$ the impurity/bath annihilation and creation operators, interaction U , hybridization strength V and chemical potential μ . Solving this model exactly and within the G_0W_0 approximation yields for the impurity self-energy

$$\Sigma_{exact}(z) = \frac{U^2}{8} \left(\frac{1}{z - 3V} + \frac{1}{z + 3V} \right) \quad (2)$$

$$\Sigma_{G_0W_0}(z) = \frac{U^2}{4a} \left(\frac{1}{z - V(2a + 1)} + \frac{1}{z + V(2a + 1)} \right), \quad (3)$$

with $a = \sqrt{1 + U/(2V)}$. Both results qualitatively agree, but G_0W_0 does not capture the correct position and weight of the two peaks in Σ . We note, however, that for $U/V \rightarrow 0$ the peak position is correctly reproduced

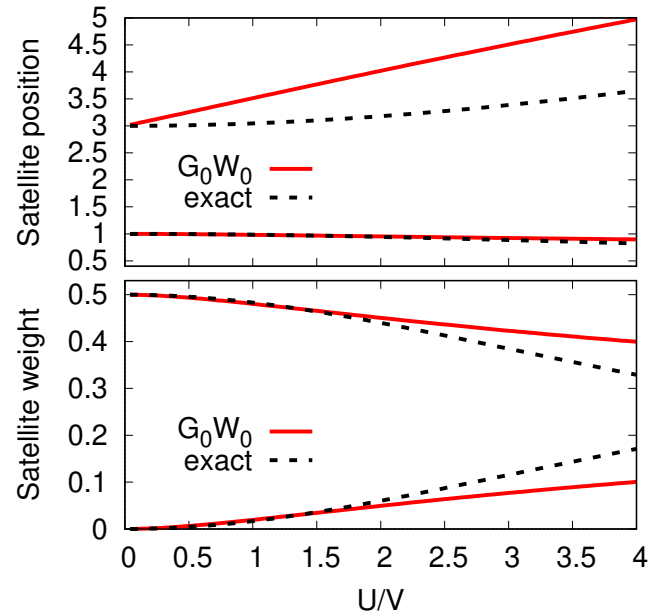


FIG. 3: The satellite positions and weights for the DMFT impurity model with one bath site as shown in Fig.2, as a function of the interaction strength U for fixed hybridization $V = 1$.

in G_0W_0 , while the weight differs by a factor of 2. In Fig.2 we show the resulting spectral function for different values of the hybridization V for fixed interaction $U = 2$. Except in the strong interaction limit $V \rightarrow 0$ G_0W_0 captures all qualitative features and correlation satellites, albeit overestimating their energetic position. This can be seen explicitly in Fig.3, where we show the position and weights of the two different satellites emerging in the spectral function as a function of the interaction strength U . G_0W_0 performs reasonably well for small values of the interaction strength $U/V \lesssim 1.5$, in particular for the bonding/antibonding states and satellite weights. The emergence of the correlation satellites in G_0W_0 , which in this setup appear as Hubbard satellites, is in fact not surprising, since a perturbative approach such as the G_0W_0 approximation is expected to become more accurate in the weakly correlated regime. If Hubbard satellites in this regime are present, it is expected that G_0W_0 is able to qualitatively capture them, as shown above.

SEPARATION OF HUBBARD SATELLITES

Previously it had been suggested to use the energetic separation of the unoccupied and occupied satellites, and their dependence on the bandwidth to distinguish plasmon satellites from Hubbard satellites[8, 9]. In the atomic limit Hubbard satellites are separated by the static onsite interaction $U(0)$, but for metallic systems a finite bandwidth enhances the separation of the Hub-

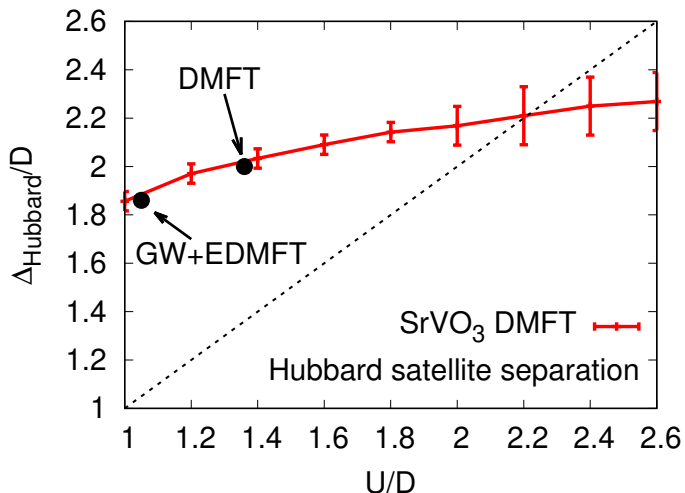


FIG. 4: The separation of the Hubbard satellites in SrVO₃ within a DMFT approach for different values of the interaction U , relative to the non-interacting bandwidth D . For small interactions the separation is much larger than the value of U , but becomes smaller for larger interactions. The non-interacting bandwidth for GW+EDMFT is given by the spectral function where the local self-energy has been removed (≈ 3.25 eV). The error bars indicate the uncertainty from analytic continuation.

bard satellites[10]. In systems far away from half-filling such as SrVO₃, the position of the Hubbard satellites is further complicated by the breaking of particle-hole symmetry. Already at the DMFT level, the separation of the Hubbard satellites $\Delta_{Hub} \approx 5$ eV greatly surpasses the value of the static interaction $U \approx 3.5$ eV.

In Fig.4 we show the dependence of the Hubbard satellite separation in SrVO₃ on the interaction U , obtained from a DMFT calculation. Up to moderate correlations (for a filling of $n = 1/6$) the Hubbard satellite separation exceeds the value of U by almost a factor of 2. On the other hand, for stronger interactions when the quasiparticle peak is close to vanishing the situation reverses and the separation becomes smaller than U . For the case of the GW+EDMFT result, which has a larger 'non-interacting' bandwidth D due to the removal of the exchange-correlation potential and non-local GW contributions[11], the Hubbard satellite separation is larger than in standard DMFT, but is well within the expected range, considering the value of $U(0)/D$ (see label 'GW+EDMFT' in Fig.4). Therefore, the Hubbard satellite separation alone is not a good quantifier to distinguish plasmonic from Hubbard satellites, as in metallic systems and systems away from half-filling, the Hubbard satellite separation significantly differs from the usual $\Delta_{Hub} \sim U$ behavior.

ONE-ORBITAL MODEL FOR PLASMONIC AND HUBBARD SATELLITES

In order to distinguish satellites of plasmonic origin and that arising from strong electronic correlations, we consider a simple model that describes the coupling of electrons to a single bosonic degree of freedom, namely the Hubbard-Holstein model

$$H = - \sum_{ij} t_{ij} c_{i\sigma}^\dagger c_{j\sigma} + U_{bare} \sum_i n_{i\uparrow} n_{i\downarrow} + \omega_0 \sum_i b_i^\dagger b_i + \lambda \sum_i n_i (b_i^\dagger + b_i), \quad (4)$$

where t_{ij} is the hopping amplitude, U_{bare} is the local instantaneous Coulomb repulsion, ω_0 is the energy of the bosonic mode (plasma frequency), generated by the bosonic annihilation and creation operators b_i^\dagger, b_i . The coupling strength between the electronic charge n_i and the bosonic mode is given by λ .

Integrating out the bosonic degrees of freedom gives rise to an effective dynamical interaction $U(\omega)$, where the coupling to the bosonic mode is now encoded in the frequency dependence

$$\text{Re } U_{\text{eff}}(\omega) = U_{bare} - 2\lambda^2 \frac{\omega_0}{\omega_0^2 - \omega^2} \quad (5)$$

$$\text{Im } U_{\text{eff}}(\omega) = -\lambda^2 \pi (\delta(\omega - \omega_0) - \delta(\omega + \omega_0)). \quad (6)$$

This model is an extension of the standard Hubbard model, and it has been shown that this model exhibits plasmonic replicas of the quasi-particle structure at multiples of the plasma frequency ω_0 , that originate from plasmonic charge excitations[12, 13].

We use extended dynamical mean-field theory (EDMFT) to solve the model at half-filling on the Bethe lattice with bandwidth $W = 4$ eV, inverse temperature $\beta = 40$ 1/eV, and a single bosonic mode $\omega_0 = 5$ eV and $\lambda = 3.5$ eV. The spectral function and Selfenergy for different values of the static interaction $U(\omega)$ is shown in Fig. 5. We observe the Hubbard satellite to completely vanish when reducing the interaction by a constant shift, where the quasiparticle peak recovers a renormalized semicircular form that corresponds to the original non-interacting dispersion on the Bethe lattice, renormalized only by the transfer of spectral weight into plasmon satellites. This behavior is even more evident in the imaginary part of the Selfenergy in Fig. 5 b). The low-energy peak responsible for the Hubbard satellite is completely suppressed for vanishing $U(0)$, while the effect on the plasmonic peaks is small. This confirms that the reduction of the interaction by a constant shift is only effecting the plasmon satellites to a minor degree, as they originate from the frequency dependence in $U(\omega)$. On the other hand, the Hubbard satellites completely vanish at $U(\omega) = 0$, allowing for a systematic classification of the nature of the satellites.

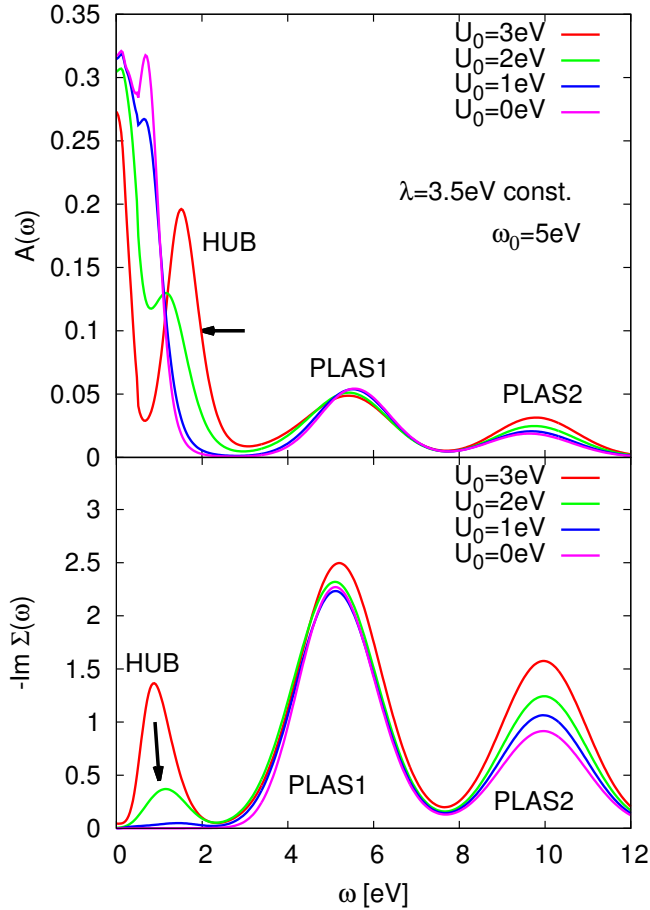


FIG. 5: The spectral function and imaginary part of the Self-energy for the half-filled Hubbard model with a one boson screening mode. We show only positive energies since the spectrum is particle-hole symmetric. The frequency dependence of the effective interaction $U(\omega)$ has been fixed with $U(\infty) - U(0) = 5$ eV, but a static shift has been applied in order to reduce the strength of the interaction but keep the transfer of spectral weight due to the bosonic coupling constant. The bosonic energy is $\omega_0 = 5$ eV, giving rise to plasmonic replica at multiples of ω_0 . We observe a disappearance of the Hubbard satellite as $U(0)$ approaches zero, while the plasmonic satellites stay mostly unchanged.

* steffen-backes@g.ecc.u-tokyo.ac.jp

- [1] B. P. S. M. G K H, K. D, and L. J, Karlheinz Schwarz, Techn. Universität Wien, Austria (2001).
- [2] H. Jiang, R. I. Gómez-Abal, X. Li, C. Meisenbichler, C. Ambrosch-Draxl, , and M. Scheffler, Computer Phys. Commun.,184, 348 **184**, 348 (2012).
- [3] A. Gaenko, A. Antipov, G. Carcassi, T. Chen, X. Chen, Q. Dong, L. Gamper, J. Gukelberger, R. Igarashi, S. Isakov, M. Könz, J. LeBlanc, R. Levy, P. Ma, J. Paki, H. Shinaoka, S. Todo, M. Troyer, and E. Gull, Computer Physics Communications **213**, 235 (2017).
- [4] R. Levy, J. LeBlanc, and E. Gull, Computer Physics Communications **215**, 149 (2017).
- [5] E. Lange, Modern Physics Letters B **12**, 915 (1998).
- [6] R. Bulla and M. Potthoff, The European Physical Journal B **13**, 257 (2000).
- [7] M. Potthoff, Phys. Rev. B **64**, 165114 (2001).
- [8] L. Boehnke, F. Nilsson, F. Aryasetiawan, and P. Werner, Phys. Rev. B **94**, 201106(R) (2016).
- [9] F. Nilsson, L. Boehnke, P. Werner, and F. Aryasetiawan, Phys. Rev. Materials **1**, 043803 (2017).
- [10] D. V. Evtushinsky, M. Aichhorn, Z.-H. L. Y. Sassa, J. Maletz, T. Wolf, A. N. Yaresko, S. Biermann, S. V. Borisenko, and B. Buchner, arxiv.org **arXiv:1612.02313** (2016).
- [11] J. M. Tomczak, M. Casula, T. Miyake, and S. Biermann, Phys. Rev. B **90**, 165138 (2014).
- [12] P. Werner and A. J. Millis, Phys. Rev. Lett. **104**, 146401 (2010).
- [13] M. Casula, A. Rubtsov, and S. Biermann, Phys. Rev. B **85**, 035115 (2012).